Supporting Information

Facile Synthesize of Pyrite (FeS_2/C) nanoparticles as Electrode Material for Non-Aqueous Hybrid Electrochemical Capacitors

*Duong Tung Pham †, Joseph Paul Baboo†, Jinju Song, Sungjin Kim, Jeonggeun Jo, Vinod Mathew, Muhammad Hilmy Alfaruqi, Balaji Sambandam and Jaekook Kim**

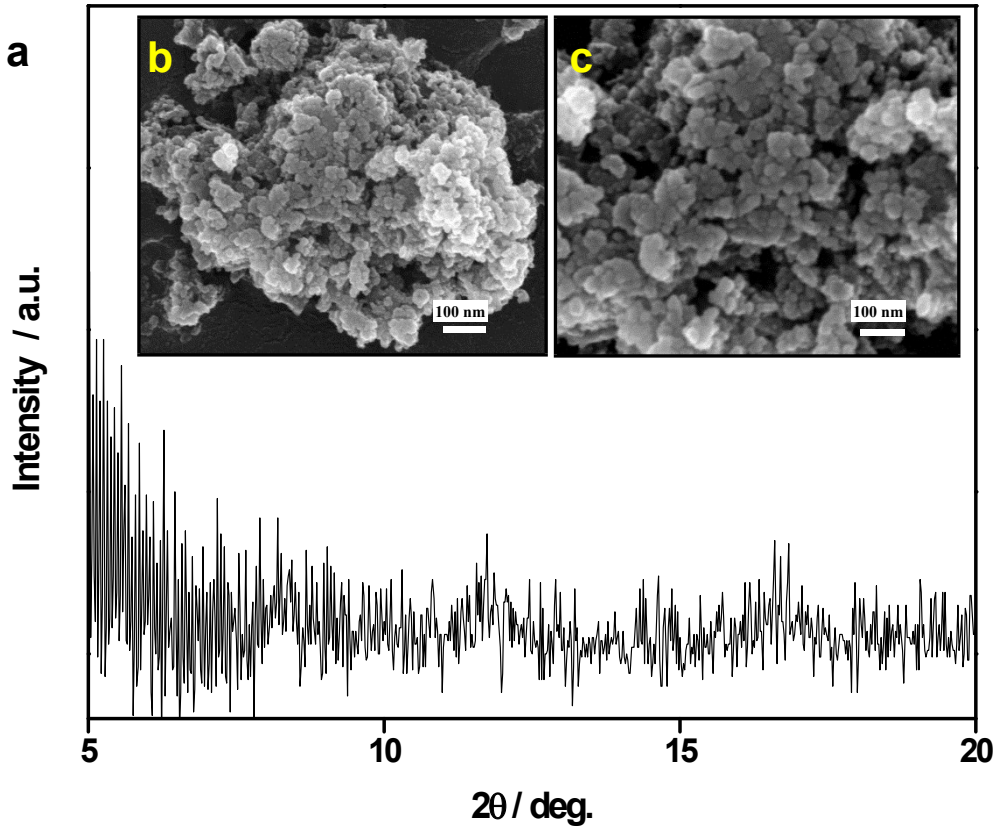

Fig. S1 (a) X-ray diffraction (XRD) pattern, (b) low and (c) high magnified FE-SEM image of the synthesized Fe-MOF intermediate sample.

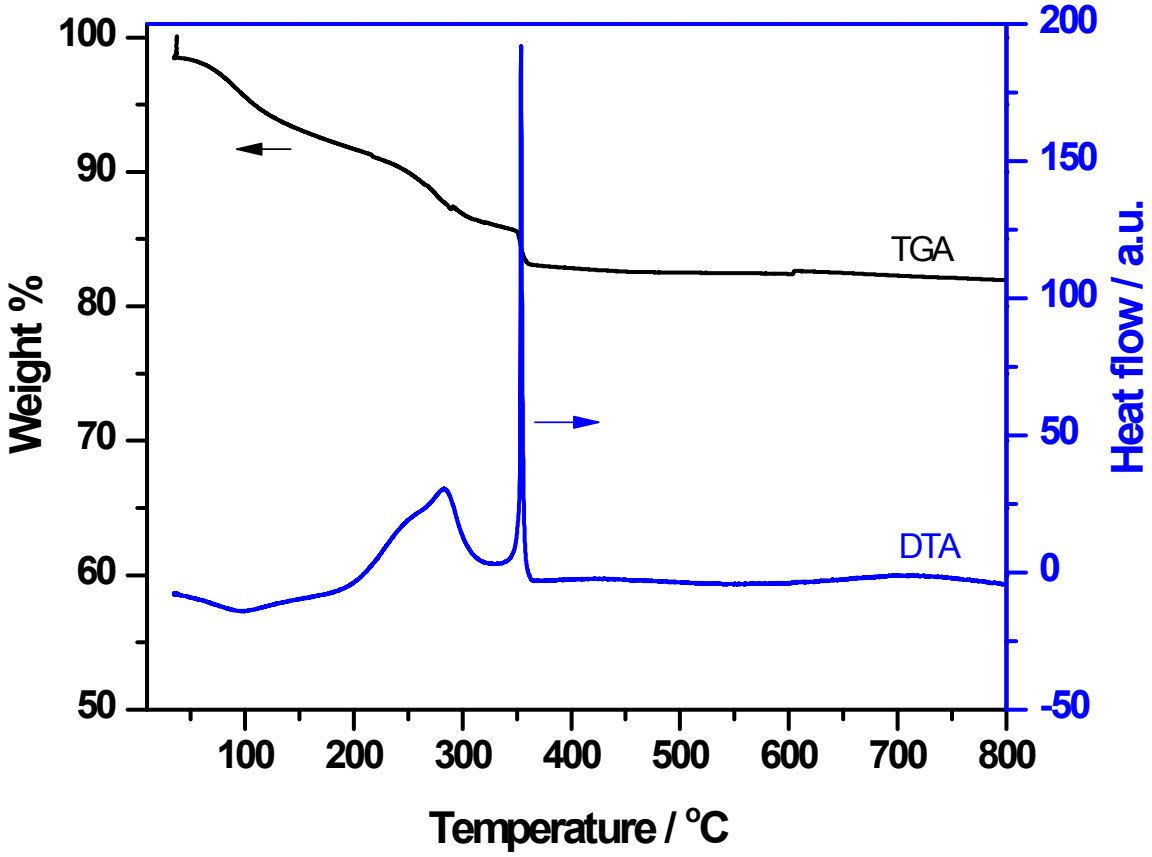

Fig. S2 TG/DTA curve of Fe-MOF precursor sample.

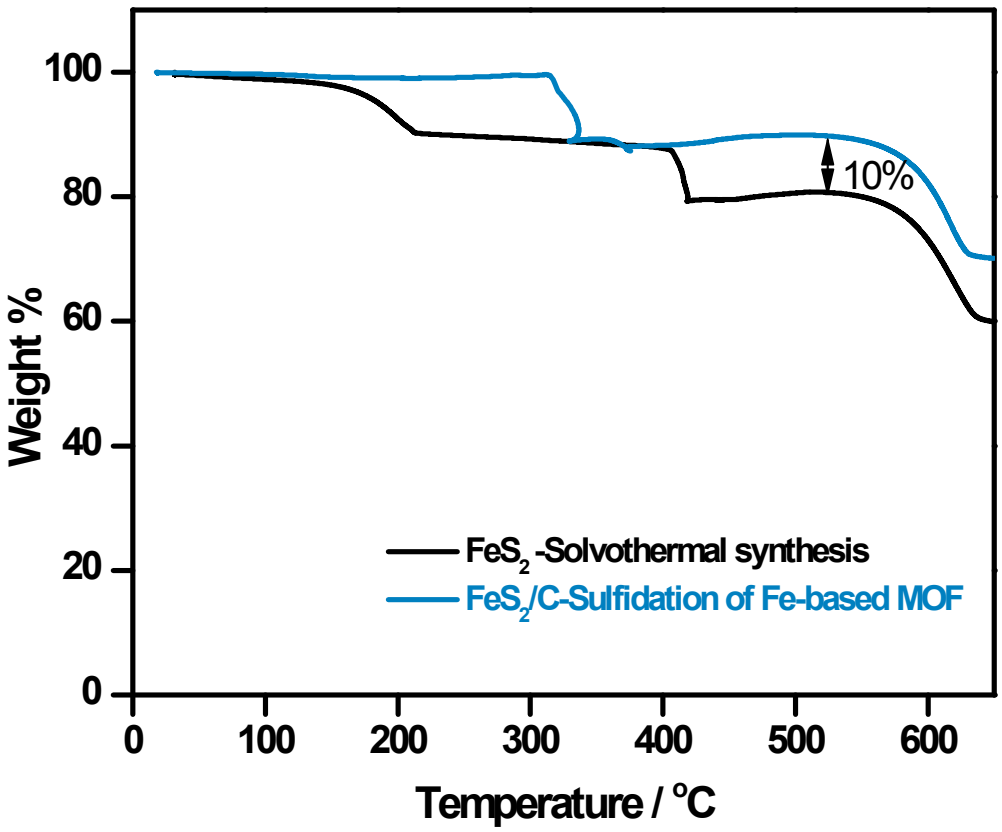

Fig. S3 (a) TGA profiles of FeS_2/C samples prepared using different methods namely solvothermal synthesis and sulfidation of Fe-MOF.

The TGA curves obtained for FeS_2 samples prepared using different methods namely solvothermal synthesis (using ethylene glycol as solvent) and sulfidation of Fe-MOF are shown Fig. S3. The initial weight loss in the temperature region ≤ 420 °C might be attributed to the removal of water molecules adsorbed on the surface of the particle and decomposition of organic compounds from the Fe-MOF precursor sample. In comparison to the solvothermal synthesized FeS_2 sample, the difference of ~10% weight loss in the temperature range 400–600 °C is attributed to the presence of carbon in the FeS_2/C sample synthesized via sulfidation.

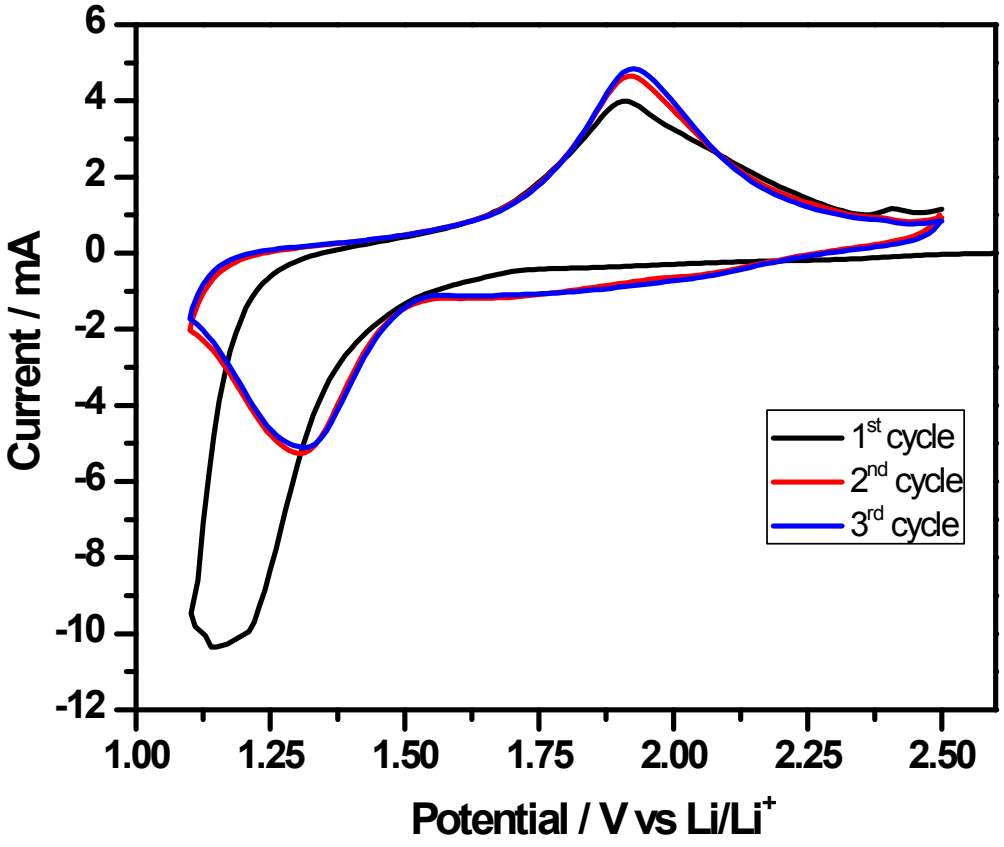

Fig. S4 Initial few cyclic voltammetry curves of FeS_2/C electrode at 0.5 mV s^{-1} scan rates in a Li||FeS_2 half-cell from 1.1 to 2.5 V vs. Li/Li^+.

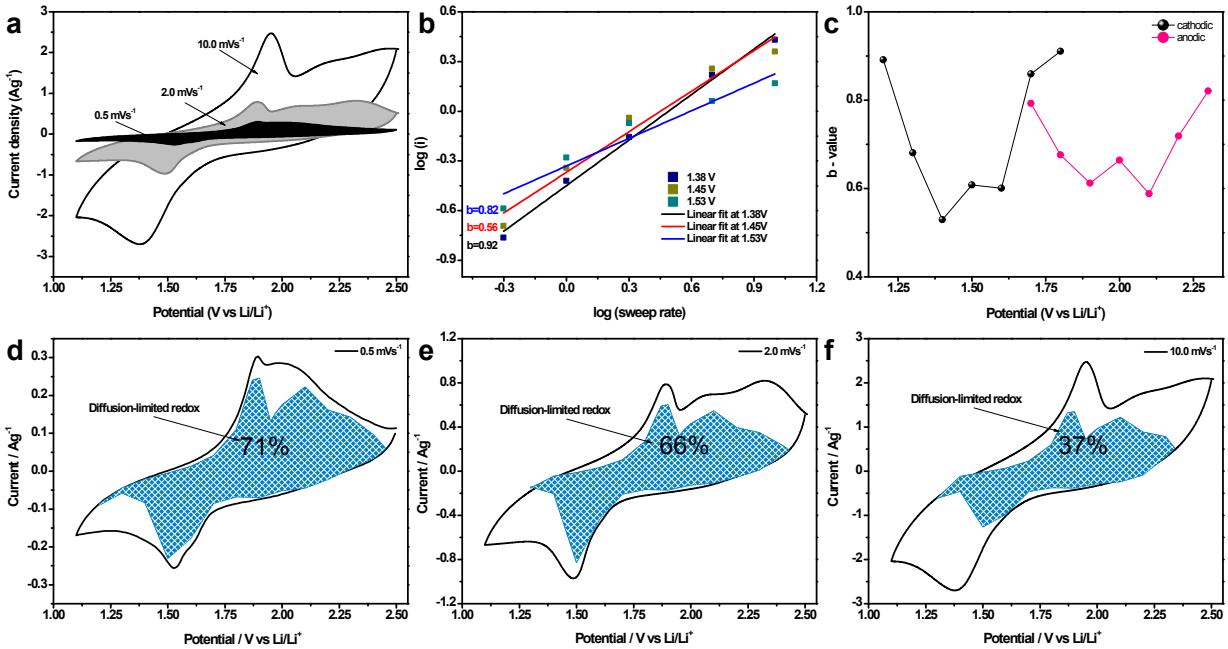

Fig. S5 (a) Cyclic voltammetry curve at specific scan rates namely 0.5, 2 and 10 mV s^{-1}, (b) log *i* versus log ν plot, (c) variations in b values near reduction/oxidation potentials (1.3/1.5 V) and (d-f) comparative plots of capacitive and diffusion limited contributions at different scan rates.

The charge storage contribution from surface capacitive effect and diffusion controlled Li-ion insertion into the bulk region of the particle was investigated by analyzing the cyclic voltammetry data at specific scan rates namely 0.5, 2 and 10 mV s^{-1} (shown in Fig. S5). The measured current (*i*) at different scan rates (ν) obeys the power law relationship[1–3]:

$$i = a\nu^b \qquad (1)$$

where a and b are adjustable parameters. Fig. S5(b) shows the linear plot of log *i* vs log ν plot at specific discharge voltages namely 1.3 and 1.5 V. The corresponding b values at specific voltages are determined from the slope of log *i* versus log ν plot (Fig. S5(b)). The overall variations in b values near reduction/oxidation potentials are shown in Fig. S5(c). In general, b = 0.5 indicates the diffusion limited process and b = 1 indicates the non-diffusion limited process. The b values gradually reduced towards 0.5 near the reduction/oxidations potential (1.4/2.0 V) and then gradually increased towards unity at the remaining potential regions.

For a capacitive behavior, the peak current is proportional to sweep rate[1]

$$i = \nu C_d A = K_1\nu \qquad (2)$$

On the other hand, for diffusion controlled insertion reaction[1]

$$i = \eta FA\, C^* D^{\frac{1}{2}}\nu^{\frac{1}{2}}\left(\frac{\alpha nF}{RT}\right)^{\frac{1}{2}}\pi^{\frac{1}{2}}\chi(bt) = K_2\nu^{\frac{1}{2}} \qquad (3)$$

where C∗ is the surface concentration of the electrode material, α is the charge transfer coefficient, D is the chemical diffusion coefficient, n is the number of electrons involved in the electrode reaction, A is the surface area of the electrode materials, F is the faraday constant, R is the molar gas constant, T is the temperature and $\chi(bt)$ function represents the normalized current for a totally irreversible system as indicated by cyclic voltammetric response.

The current response at a fixed potential can be the combination of both the surface capacitive and diffusion controlled insertion mechanisms[1,3]:

$$i = K_1\nu + K_2\nu^{\frac{1}{2}} \qquad (4)$$

The capacitive contributions at each potential was also determined using equation DD[1]

$$\frac{i}{\nu^{\frac{1}{2}}} = K_1\nu^{\frac{1}{2}} + K_1 \qquad (5)$$

where K_1 and K_2 could be determined from the slope and y-intercept of $i\nu^{-1/2}$vs $\nu^{1/2}$ plot with respect to various scan rates at that specific potential. Substituting K_1 and K_2 at specific potential in equation A and B we can determine the contribution of surface capacitive and diffusion limited process at that specific sweep rate. The comparative plot of capacitive and diffusion limited contributions at different scan rates are shown in Fig. S5(d-f). The contribution from diffusion limited process decreased from 71 % at lower scan rate (0.5 mV S^{-1}) to 37% at higher scan rate (10 mV S^{-1}).

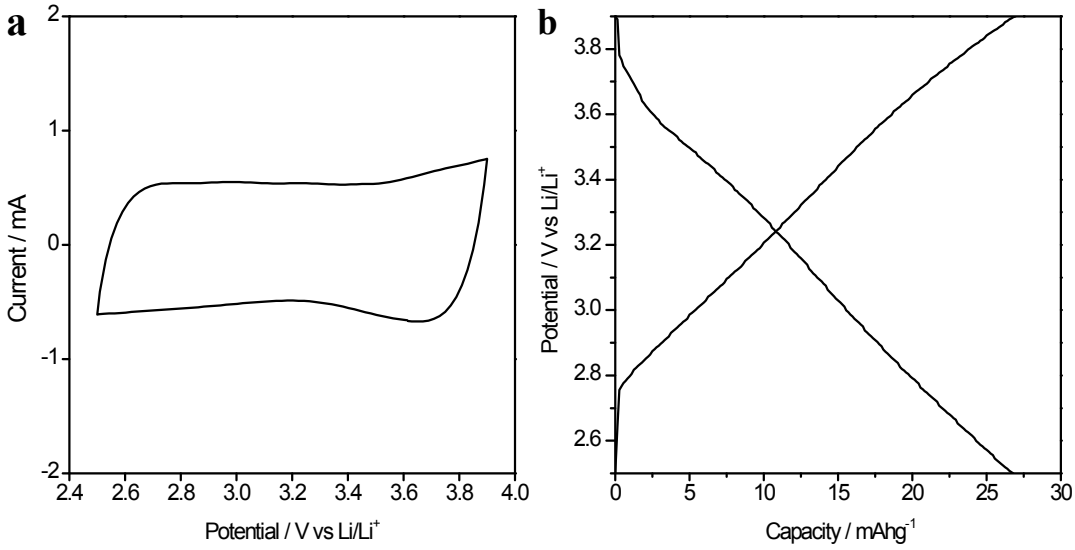

Fig. S6 (a) Cyclic voltammetry curve at 1 mV s^{-1} and galvanostatic charge/discharge curve at 0.5 A g^{-1} of Li||AC half-cell from 2.5 to 3.9 V vs. Li/Li^+.

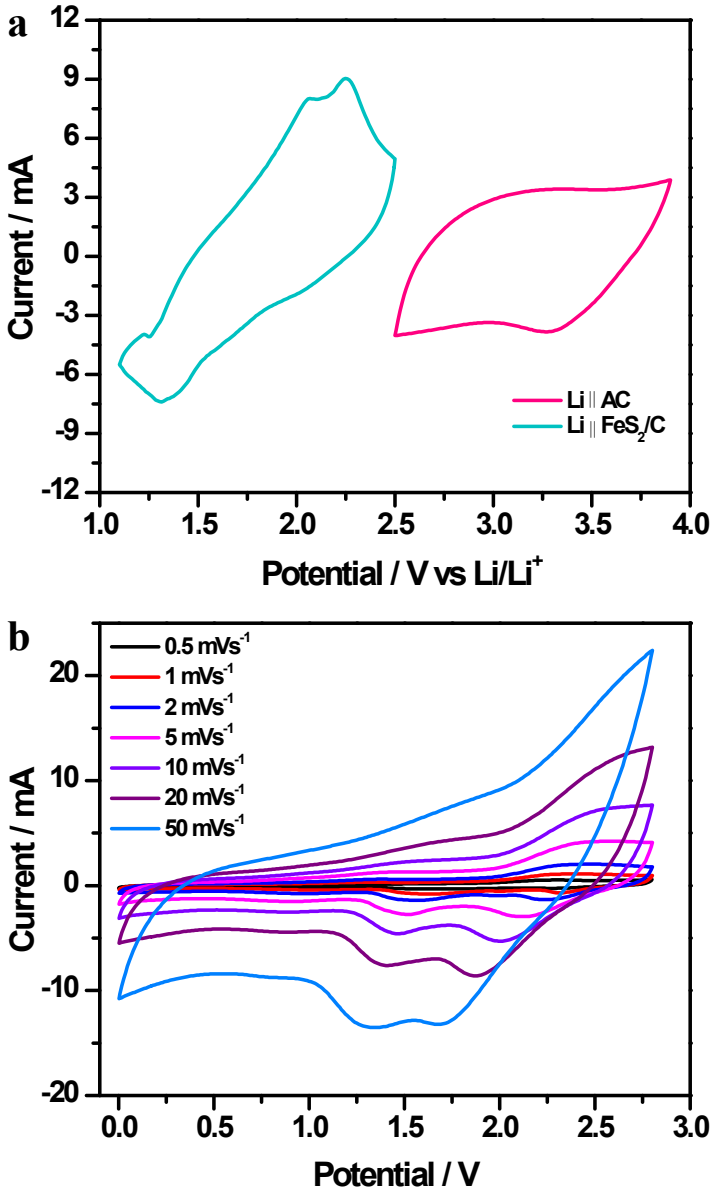

Fig. S7 Cyclic voltammograms of (a) Li||FeS_2/C half-cell and Li||AC half-cell at 0.5 mV s^{-1} and (b) FeS_2/C||AC (NHEC) in the working potential window 0 – 2.8 V at various scan rates.

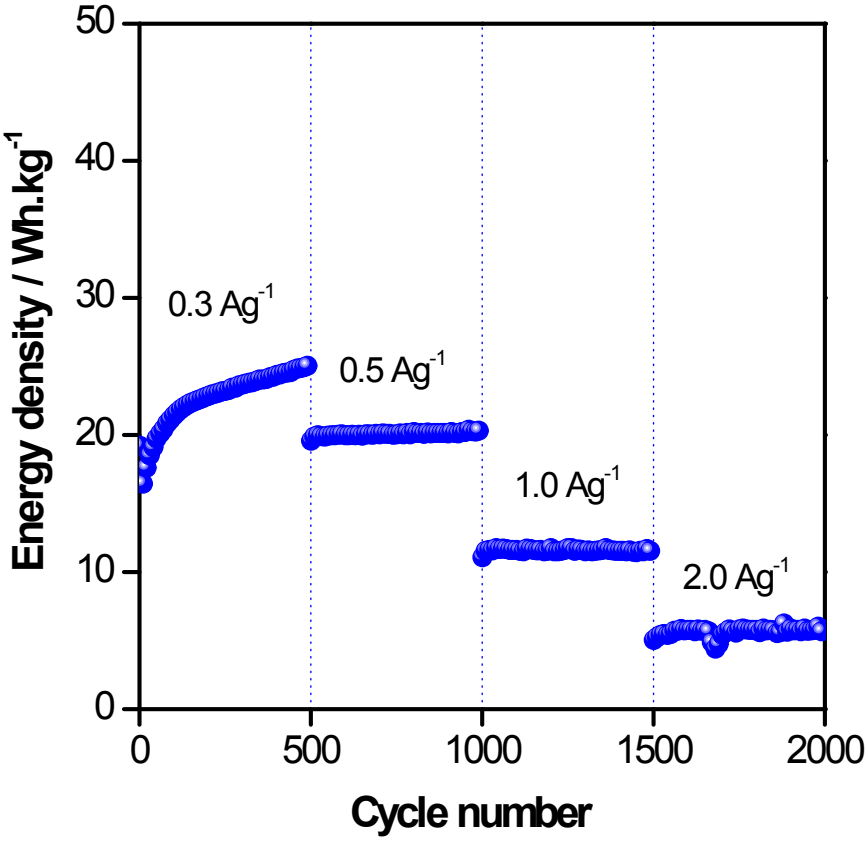

Fig. S8 Specific energy density of FeS_2||AC NHEC in the working potential window (a) 0 – 2.8 V as a function of different current densities.

Reference

1 J. Wang, J. Polleux, J. Lim and B. Dunn, *J. Phys. Chem. C*, 2007, **111**, 14925–14931.

2 M. Sathiya, A. S. Prakash, K. Ramesha, J. M. Tarascon and A. K. Shukla, *J. Am. Chem. Soc.*, 2011, **133**, 16291–16299.

3 T. Brezesinski, J. Wang, J. Polleux, B. Dunn and S. H. Tolbert, *J. Am. Chem. Soc.*, 2009, 1802–1809.